

Purdue University

Purdue e-Pubs

---

International Refrigeration and Air Conditioning  
Conference

School of Mechanical Engineering

---

2022

## An Experimental Method To Determine The Contact Thermal Resistance Of PCM Materials Undergoing Large Volume Change

Joseph Rendall

Zhenglai Shen

Som Shrestha

Tony Gehl

Jerald Atchley

Follow this and additional works at: <https://docs.lib.purdue.edu/iracc>

---

Rendall, Joseph; Shen, Zhenglai; Shrestha, Som; Gehl, Tony; and Atchley, Jerald, "An Experimental Method To Determine The Contact Thermal Resistance Of PCM Materials Undergoing Large Volume Change" (2022). *International Refrigeration and Air Conditioning Conference*. Paper 2486.  
<https://docs.lib.purdue.edu/iracc/2486>

This document has been made available through Purdue e-Pubs, a service of the Purdue University Libraries. Please contact [epubs@purdue.edu](mailto:epubs@purdue.edu) for additional information. Complete proceedings may be acquired in print and on CD-ROM directly from the Ray W. Herrick Laboratories at <https://engineering.purdue.edu/Herrick/Events/orderlit.html>

## An experimental method to determine the contact thermal resistance of PCM materials undergoing large volume change

Joseph RENDALL<sup>1\*</sup>, Zhenglai SHEN<sup>1</sup>, Som SHRESTHA<sup>1</sup>, Tony GEHL<sup>1</sup>, Jerald ATCHLEY<sup>1</sup>,

<sup>1</sup>Oak Ridge National Laboratory, Buildings and Transportation Science Division,  
Oak Ridge National Laboratory, Tennessee, USA  
Contact Information ((865) 341-0422, rendalljd@ornl.gov)

### ABSTRACT

Contact resistance between heat exchangers and phase change materials (PCMs) influences the overall thermal conductivity of thermal energy storage system (TES) and cannot be ignored when PCMs experience large volume changes during phase change. In this paper, a heat flow meter apparatus (HFMA) was modified to measure the contact pressure throughout the phase change process to determine the impact of this volume change. First, resistive based pressure sensors were added to the HFMA. Second, the heat flow measurements from the HFMA were used to determine the overall resistance for a baseline case without a PCM sample and to control for any temperature based effects. Third, a PCM sample was added, and the thermal contact conductivity reported as the temperature was swept in the HFMA. Finally, with all noise cleaned, a state of charge (SOC) vs. resistance reading relationship was developed. The results shown that a HFMA with the addition of a pressure measurement can determine the contact resistance and SOC of a PCM material. These results suggests that SOC models can be developed for various materials in the modified HFMA. Then, when the PCM is deployed a simple pressure sensor or deflection sensor on an expansion bladder can be used to give real time SOC information in the field. These types of pressure based sensors are advantageous as the current state of the art sensors are temperature measurements, which are only a local measurement. The pressure type measurement allows for a bulk reading of SOC. Also, when a PCM store with an expansion tank allows for insuring large enough contact pressure.

### 1. INTRODUCTION

The building sector accounts for 40% of the global energy consumption and it is predicated that an increase of 28% by 2035 (Bland, Khzouz, Statheros, & Gkanas, 2017; Khadiran, Hussein, Zainal, & Rusli, 2016; Yang, Yan, & Lam, 2014). To reduce the energy consumption of buildings and the associated CO<sub>2</sub> emissions, The U.S. Department of Energy supports the development of low-cost phase change material (PCM) and PCM based thermal energy storage (TES) system. PCM based TES system was found to be promising from the efficiency and economical point of view. The advantages of TES using PCMs include high storage density and constant temperature behavior during the phase change, allowing a high heat transfer rate compared to sensible heat transfer. More importantly, it can shift electric load for building space conditioning and therefore it has been increasingly applied in building thermal management (Cabeza, Castell, Barreneche, Gracia, & Fernández, 2011; Kalnæs & Jelle, 2015; Mavriannaki & Ampatzi, 2016; Souayfane, Fardoun, & Biwole, 2016).

The performance of latent heat storage system depends on the thermophysical properties of PCM, the design of heat exchanger, and the contact thermal resistance between them. Commonly used PCMs for building thermal energy storage mainly include organic PCMs, inorganic PCMs, and eutectic PCMs (Kenisarin, 2014). Organic PCMs have been increasingly studied because of their relatively high latent heat capacity, appropriate phase-transition temperature, stable physical and chemical characteristics, non-corrosive, and congruent melting. However, pure organic PCMs show some shortcomings which may limit their usage, including low thermal conductivity (usually less than 0.2 W/m<sup>2</sup>K (Fang et al., 2014)), high volume variation and liquid seepage during stage changes (Mehrali et

Notice: This manuscript has been authored by UT-Battelle, LLC under Contract No. DE-AC05-00OR22725 with the US Department of Energy. The United States Government retains and the publisher, by accepting the article for publication, acknowledges that the United States Government retains a non-exclusive, paid-up, irrevocable, worldwide license to publish or reproduce the published form of this manuscript, or allow others to do so, for United States Government purposes. The Department of Energy will provide public access to these results of federally sponsored research in accordance with the DOE Public Access Plan (<http://energy.gov/downloads/doe-public-access-plan>).

al., 2014). Organic PCMs can be categorized as paraffin organic PCMs and non-paraffin organic PCMs. Paraffin is composed of a straight chain alkane mixture. The range of a paraffin's melting point is from  $-12^{\circ}\text{C}$  to  $71^{\circ}\text{C}$  and they can store 128 kJ/kg to 198 kJ/kg of heat (Peng, Fuchs, & Wirtz, 2004). Paraffin materials are one of the most popular PCMs used because they are non-corrosive and non-subcooling. In addition, paraffin materials are stable and experience relatively small volume changes during phase change. However, they have a relatively low thermal conductivity (usually 0.21-0.24 W/mK) which may limit their application for thermal energy storage applications (Kamali, 2014; Lachheb, Karkri, Albouchi, Mzali, & Nasrallah, 2014). Non-paraffin PCMs includes alcohols, esters, glycols and fatty acids, which have a variety of properties and is in intensively research (Kenisarin, 2014). Since paraffin were used in most commercially available organic PCMs, the pros and cons of non-paraffin organic PCMs were not detailed here. Inorganic PCMs usually have higher heat of fusion per unit mass with lower cost. The mostly used inorganic PCM is salt hydrates, which are a category of inorganic salts containing one or multiple water molecules. They suffer from super cooling phase segregation, lack of thermal stability, corrosion, and decomposition (Baetens, Jelle, & Gustavsen, 2010; Fauzi, Metselaar, Mahlia, & Silakhori, 2014; Tyagi & Buddhi, 2007). Therefore, thermal energy storage system should be carefully designed to deliver the desired properties when using hydrated salts. Eutectic PCMs are the combination of at least two other PCMs. The purpose of developing eutectic PCM is mainly to combine the advantages of different PCMs. For example, the combination of organic and inorganic PCM may lead to higher thermal conductivity than the constitute organic PCM while having reduced cost. For more details related to eutectic PCMs, please see the review works of Singh et al. (Singh et al., 2021).

PCM based heat exchangers can be broadly divided into traditional shell and tube heat exchangers and finned heat exchangers. Depending on the placement of PCM and number of tubes, shell and tube heat exchangers can be further divided into cylinder mode, multi-tube model and pipe model (Kalapala & Devanuri, 2018). In cylinder model PCM is placed in the shell and heat transfer fluid (HTF) passes through the inner tube, while the multi-tube model consists of more than one tube. It is noted that the cylinder model is the most considered type of heat exchanger for latent heat storage systems due to its simplicity (Agyenim, Hewitt, Eames, & Smyth, 2010). In the pipe model, PCM is placed in inner tube and HTF passes through the annulus. To increase the heat transfer efficiency, finned heat exchangers were attracted more research interest recently (Abdulateef, Mat, Abdulateef, Sopian, & Al-Abidi, 2018). Different types of fins were used which includes longitudinal fins, circular/annular fins, and plate fins. For example, Rahimi et al. (Rahimi et al., 2014) experimentally investigated the melting and solidification of PCM (RT35) in a plate finned tube heat exchanger. The results showed that fins lead to more uniform average temperature distribution regardless of the flow regime. In addition, some novel PCM heat exchangers were developed recently. For instance, Lin et al. developed a novel PCM heat exchanger that could be used for storing warm and cold water supplied from the anisotropic wall (Lin, Zhang, Ling, Fang, & Zhang, 2020). The new energy storage unit is a pillow plate type heat exchanger with multi flowing channels, while the phase change material (PCM) - sodium acetate trihydrate (SAT) works as the energy storage medium. Youssef and Tassou (Youssef, Ge, & Tassou, 2018) experimentally and numerically studied the performance of a spiral-wired tubes heat exchanger and found that a solar-assisted heat pump for hot water production had a 6% to 14% increase in COP due to the integration of PCM and controls. The experimental results show that the designed system can meet the daily hot water demand with constant hot water supply.

While the thermophysical properties of PCM and the design of the heat exchanger have been studied extensively, the contact thermal resistance is seldomly studied. Experimental work conducted by Woods et al. (Woods, Mahvi, Goyal, Kozubal, & Odukamaiya, 2019) showed that contact thermal resistance could be about 50% of the total resistance to heat transfer in expanded graphite PCM composites. To date, contact thermal resistance has not been adequately modeled during the phase change of PCM with large changes in volume. Furthermore, the model developed by Woods et al. ignored volumetric changes of PCM and predicted the contact thermal resistance as about 10% of total heat transfer resistance (Woods et al., 2021), but not the 50% they later measured experimentally (Mahvi & Woods, 2020; Woods et al., 2019). Wu et al. experimentally studied the improved water heating of PCM embedded heat exchangers (Wu, Feng, Liu, & Li, 2018), and the results indicated that the volume expansion rate of a 16 L expanded graphite paraffin heat exchanger (EGPHE) was 6.25% at  $76^{\circ}\text{C}$ . A semicircular groove was used to reduce the thermal contact resistance between heat exchanger (copper pipe) and PCM. On the other hand, Merlin et al. (Merlin, Delaunay, Soto, & Traonvouez, 2016) showed thermal contact resistance could be less than 1.2% when there is tight contact between the EG-PCM and tubes carrying the heat transfer fluid. Although previous works noticed the potential importance of contact thermal resistance in TES system design, there lacks a systematically method to quantify it and correlate it with the state-of-charge (SOC) of PCM.

In this light, we present an experimental method to quantify the contact thermal resistance between PCM and heat exchanger. Specifically, a heat flow meter apparatus (HFMA) was modified to measure the thermal contact pressure and infer the state of charge throughout the phase change process of PCM by including an array of pressure sensors. To complete this work multiple experiments were undertaken in side and outside the HFMA to remove material and temperature based errors in the findings. To reduce the complexity, linear relationships were sought through experiment design and the results generally show good linearity.

## 2. METHODOLOGY

### 2.1 Experiment Apparatus

The instruments to measure the phase change dependent contact pressure for PCM materials with large volumetric change during phase transition include a Fox 305 HFMA (Instruments, 2022), 10 haptic sensors wired in parallel, and a data acquisition system (DAQ), as shown in Figure 1. The HFMA allows the characterization of insulative and PCM materials by controlling the temperature inside the device with high accuracy and measuring the heat flux into and out of the material at steady-state conditions. The Fox 305 HFMA provides extremely precise readings: 0.6 mV resolution on integrating high output heat flux transducers, 0.001" precision in thickness measurement, and 0.01°C temperature control and resolution (Instruments, 2022). The operation of this machine has been documented in Ref. (ASTM C1784-14, 2015) as well as listed on their website. The precise readings of conductivity from the HFMA was critical to obtain a highly accurate and sensitive contact pressure measurements.

This sensor was placed inside the HFMA to measure the contact pressure of PCM materials that undergo a large volumetric phase change during phase transition in conductivity-based measurements. The creation of a pressure sensor via using a series of inexpensive thin-film pressure sensors are sometimes called haptic sensors [(DFROBOT, 2022)]. Ten of these sensors were wired in parallel to determine the average pressure experienced under the HFMA test. A high-resolution CR6 DAQ system was used to create a half-bridge circuit to measure the resistance of these sensors. The standard error of the excitation voltage was  $\pm 0.02\%$  which is applied to create a  $\frac{1}{2}$  Wheatstone bridge. The sensor was sandwiched between multiple materials to ensure good reading. It includes a layer of highly conductive copper plate, a layer of silicon plastic pads, and a layer of high conductivity flexible material such as thermal pads for CPU heat sinks. The copper plate was used to spread the heat evenly through the sensor. The sensor was then attached to the copper plate with a layer of silicon plastic pads to protect the electronics on its top surface. Lastly, it was topped with a flexible material that engaged the haptic sensor for the baseline test. The PCM test includes adding a vacuum-sealed bag of PCM on top of this material stack – 414 grams of Pure Temp 15 was used in the PCM test.

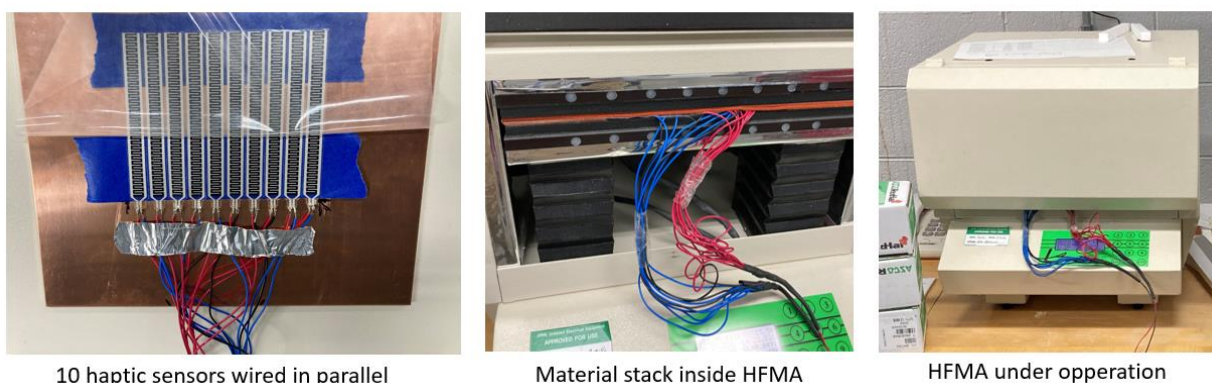


**Figure 1:** Experimental instrumentation

### 2.2 Experiment Procedure and Uncertainty

The experiment includes three major steps, i.e., 1) determine the pressure the HFMA can provide by altering a potentiometer inside the machine which controls four motors close to test samples; 2) determine sandwich pads materials to pair with the haptic sensor for the best reading; 3) remove any temperature dependent drift in the reading from the resistive type sensors; 4) determine the conductivity of the baseline material stack; 5) calculate the contact conductivity in the baseline test; 6) add PCM to the material stack inside the HFMA and calculate the change in contact conductivity as the HFMA works through a temperature range and 7) determine the relationship of resistive reading to state of charge for the PCM at its phase change temperature.

To characterize the pressure applied by the HFMA a couple flexible materials were tried to determine the pressure applied by the HFMA. The material needed to have elastic deflection under the applied loads of HFMA in order for the thickness reading in the HFMA to also be linear. A stiff fiberglass pad was found suitable because it can withstand the pressure applied by the HFMA (0.2 to 1.2 psi) and deflect linearly. To calibrate the deflection of this material, the fiberglass was placed between stiff plastic plates, and the deflection was measured under varying loads as shown in Figure 2.

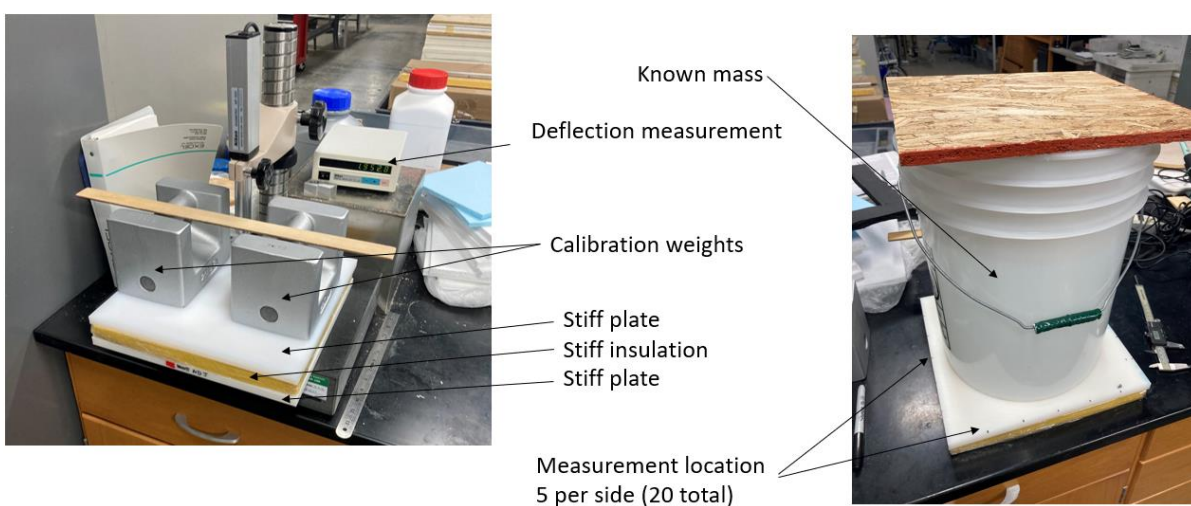


**Figure 2:** Experiments to calibrate the deflection of stiff fiberglass pad under various loads

Four calibration weights (two 25.00 lb weights, one 6.61 lb, and one 11.02 lb weight and one known mass) were used to develop the relationship between pressure and deflection. The known weight was a 5-gallon bucket of water measured on a 0.5% accurate scale to be 32.94 lb. The deflection under varying weights was measured at 20 points along the edge of the material stack.

To engage the pressure sensor a highly flexible material is required. Initially a silicone mat (Figure 3 left) was used. The limit was the thermal resistance of this material, which had a conductivity of 0.1402 W/mK and a small thickness. Some PCM samples will have higher conductivity. This precision was then replicated with a material of high enough conductivity while still being thin, to allow the HFMA to determine the thermal conductivity of the PCM material to be tested. Two thermal contact pads with 6 w/mK conductivity were chosen as to not limit the range of the material tested. Finally, a series of tests were conducted to determine the thermal drift of the ten sensors. This is discussed in more detail in the next section.

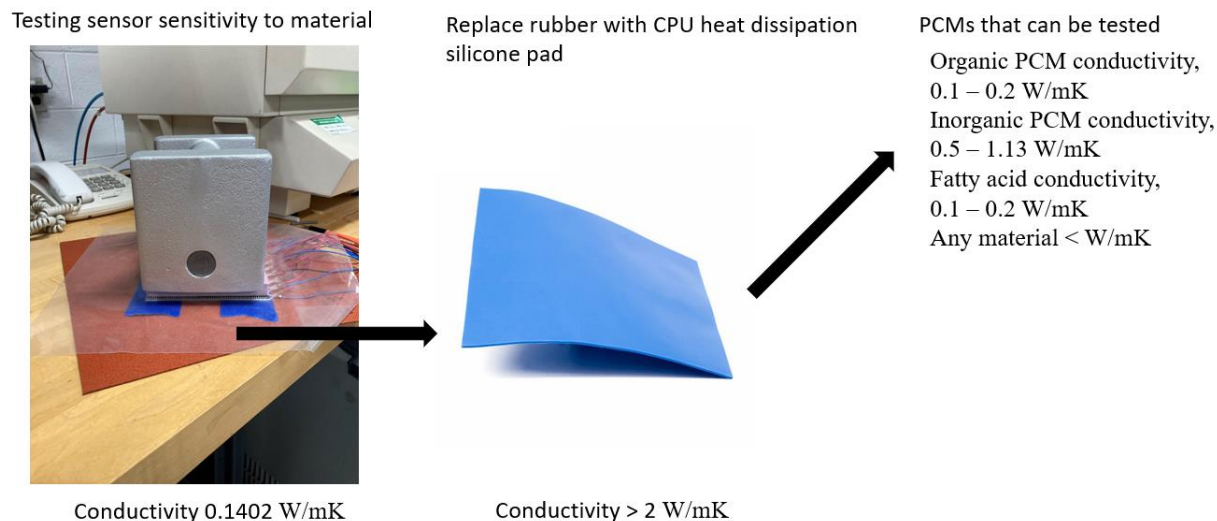


**Figure 3:** Improvement of material in contact with the pressure sensor. (left) insulative silicone mat (middle) high conductivity silicone CPU pad (right) PCMs with typical range of conductivity that can be tested due to the increase in conductivity of the material for a similar thickness.

The HFMA allows setting multiple temperatures inside the machine and stepping through these temperatures with high accuracy (e.g., < 0.5% variance in temperature and heat flux readings). A separate DAQ system was built to read the signal from the resistive sensor during this internal temperature sweep. One CPU was used to record both the resistive measurements and HFMA temperatures. This allowed the readings to be averaged by aligning the timestamps of the DAQ and HFMA output as it went through the setpoints.

### 3. RESULTS AND DISCUSSION

#### 3.1 Calibration of the pressure sensors

Early experiments showed hysteresis in loading and unloading the sample to the amount of deflection measured. Under the initial loading, before nonlinear deflection, the linearity of the behavior was quite good. When the material is sufficiently stiff, the nonlinear behaviors can be ignored. On the other hand, if the material is too stiff, the haptic sensor cannot determine a steady reading; thus, the stiffness of the material and the resistive reading are coupled. In this second stage of development, the material needed to be flexible enough for the haptic sensor to give good data.

The correlation for the applied load to the deflection of the fiberglass is shown below in Figure 4 (a). The correlation for the HFMA machine voltage to auto thickness of machine output for this fiberglass sample is shown below in Figure 4 (b). These two correlations are combined and the error in the measurements propagated together to determine the voltage applied at the HFMA to the pressure as below (Figure 4 (c)). The error was propagated in EES and is rather large due only 3 data points found in the linear region when the 304 HFMA machine was compressing the fiberglass pad. The error will be reduced by taking more data points in Figure 4 (b) before taking on experimental work that uses the correlation (i.e., starting the tests under different contact pressures).

Regardless of the first 3 correlations, a baseline test was undertaken to determine the conductivity of the material stack. The effective conductivity of the material stack increased as the temperature increased Figure 4 (d). This is likely due to the temperature dependence of the CPU pad. The contact conductivity in the test that include the PCM was later calculated by removing the conductivity temperature dependence of the material stack.

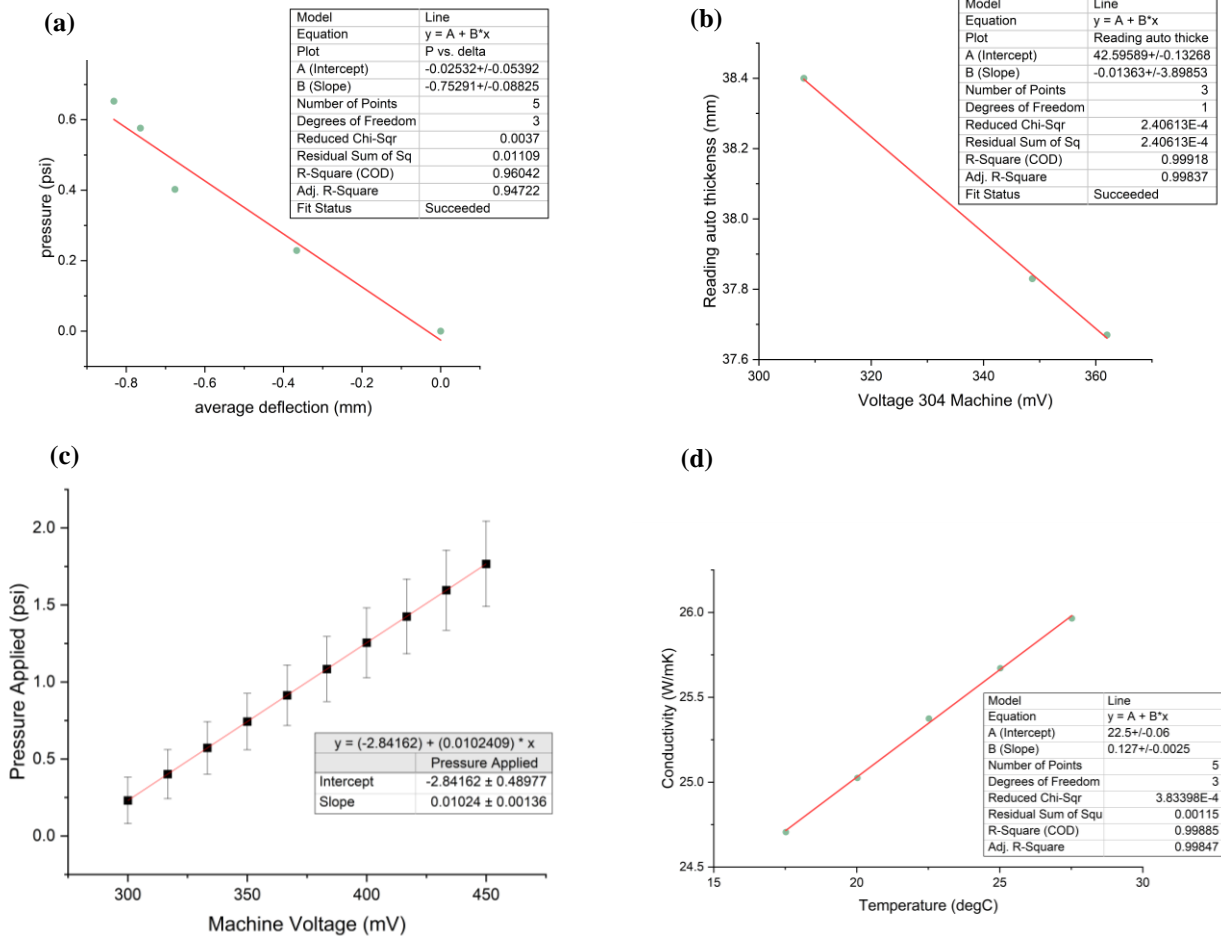


**Figure 4:** (a) Pressure applied to sample and deflection average deflection recorded (Twenty samples were taken for each data point on the graph) (b) fiberglass thickness vs. voltage read across the potentiometer in the HFMA 304 machine (c) relationship between HFMA 304 potentiometer voltage to pressure applied with error propagated (d) conductivity of the material stack vs. temperature in the baseline (no PCM) test case.

The temperature correction correlation for the sensor was determine as unnecessary. The baseline conductivity of the material stack was correlated to temperature by  $k=0.127(T)+22.5$  for the temperature range of 17.5 to 30 C with a  $R^2$  of 0.999. This conductivity difference based on temperature was removed from the conductivity measurement of the PCM by applying a 12.7% reduction in contact conductivity due to the temperature dependance of the material stack below the PCM. With one extraneous data point removed, the relationship between contact resistance and haptic sensor resistance is clear (Figure 5).

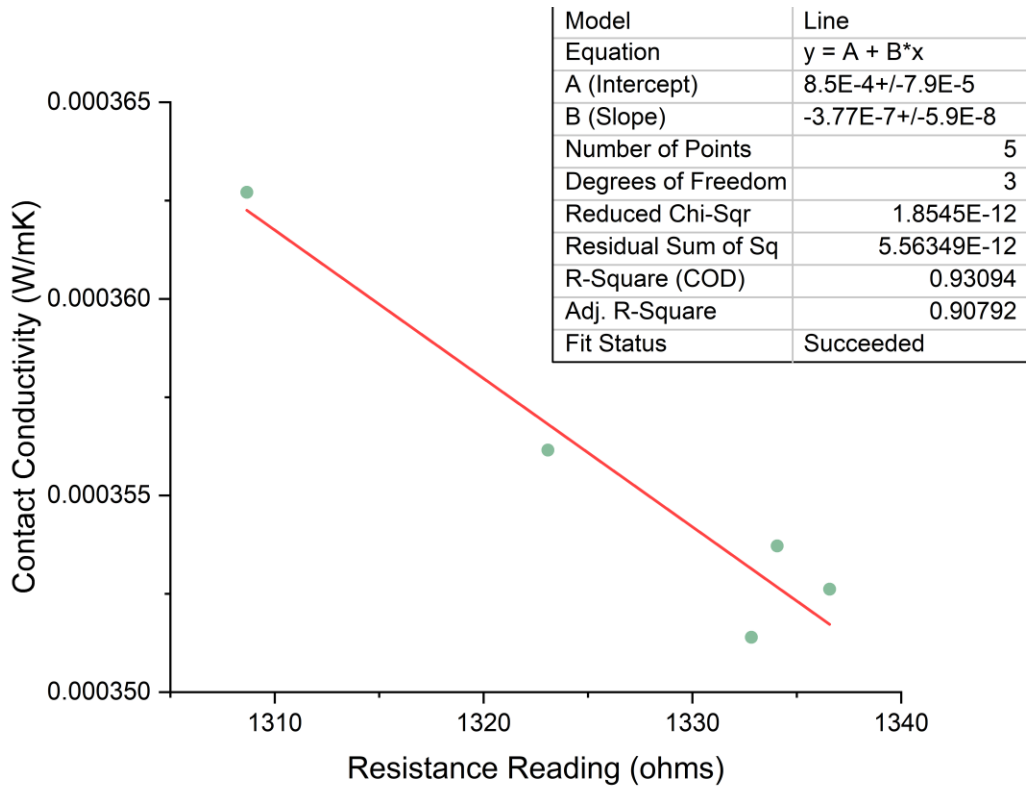


**Figure 5:** The average conductivity of the thermal contact region in the HFMA with Pure Temp 15 PCM

The contact conductivity is very low and the thickness assumed was 0.0000254 m for each of the 6 locations of contact between the materials in the sensor and the PCM. Each layer inside the HFMA will have different contact resistances and thicknesses. Since the purpose of the study was to show the relationship between the pressure sensor and the contact resistance or conductivity, the actual values calculated are less important at this point of the research.

For one sample, the state of charge was correlated to the contact conductivity from the resistance of the haptic sensor by the equation  $CC = 0.00085 - (RR)0.000000377$  (Figure 7). It should be noted, that resistance reading is very sensitive to the material in contact with the sensor. This equation only works for the high conductivity material selected for these experiments and the resistor used in the half wheat-stone bridge.

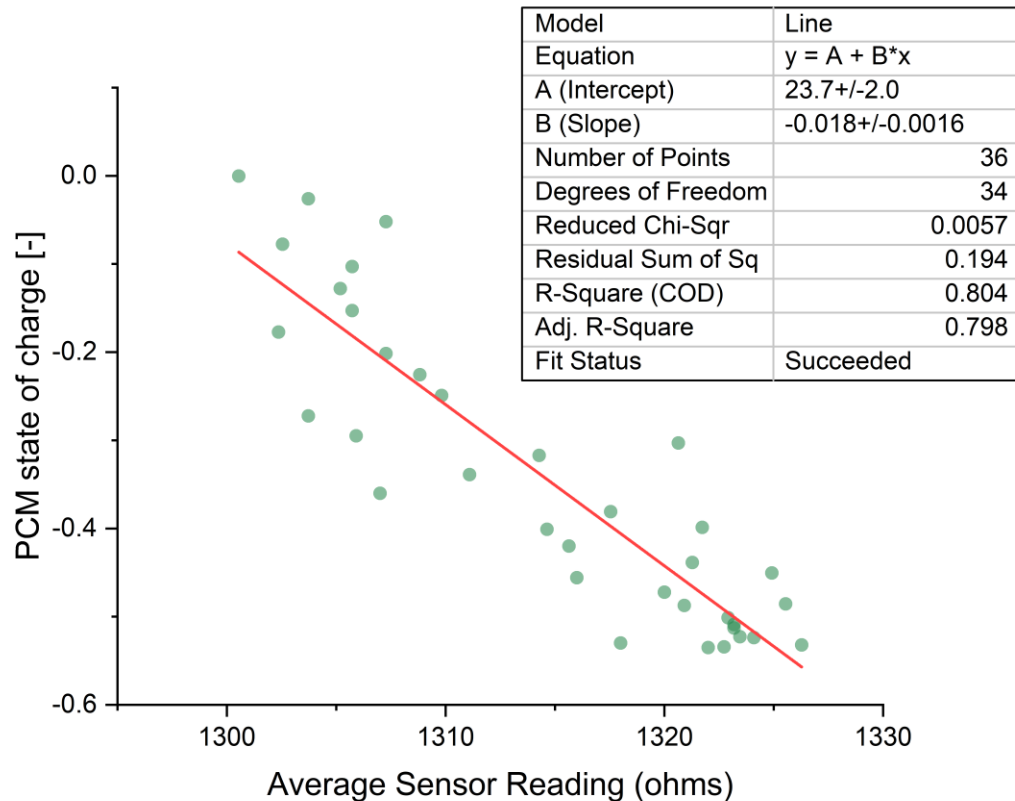


**Figure 6:** State of charge relationship to resistance read from the haptic sensors for Pure Temp 15 undergoing phase change at 15 °C

Interestingly, the HFMA applied a large heat flux in the first 11 minutes of the 10 hour experiment to freeze the sample at 15 °C. The calculated imbalance of heat flux would result in a 41% frozen PCM sample after this first block. The HFMA continued to freeze and melt the sample. A correlation between the resistance readings and the SOC calculations was present while the PCM was undergoing the freezing and melting process at constant temperature as seen in Figure 6. Additional experiments will be conducted to determine heat loss from the HFMA to confirm the SOC through the melting and freezing process for multiple PCM samples.

#### 4. CONCLUSIONS

We thank the reader for their interest in our developments. The contact resistance can be correlated to the reading from the resistive sensor with high confidence when combined with the HFMA machine. Furthermore, the state of charge can also be correlated with this same sensor setup. The absolute resistance reading is repeatable between experiments but is highly dependent on the configuration of the material stack used in conjunction with the PCM. Furthermore, plastic deformation in the material stack with the sensor will lead to a nonlinear result. The HFMA and haptic sensors created an environment in which the expansion of the PCM undergoing phase change could be adequately characterized. The results presented clearly show that as the PCM changes phase inside an enclosure the contact pressure changes and this can be used to calculate the contact conductivity and more importantly to thermal energy storage systems, the state of charge.

Finally, the concept of using a pressure sensor or an expansion tank with a deflection reading to determine the state of charge of PCM in the field is proven possible in this work. Future work will correlate resistance readings to

absolute contact pressure, develop correlations for multiple PCM materials and develop a full-scale thermal storage unit that outputs the state of charge by a simple measurement device (e.g., pressure or diaphragm deflection sensor).

## 5. REFERENCES

- Abdulateef, A. M., Mat, S., Abdulateef, J., Sopian, K., & Al-Abidi, A. A. (2018). Geometric and design parameters of fins employed for enhancing thermal energy storage systems: a review. *Renewable and Sustainable Energy Reviews*, 82(June 2017), 1620–1635. <https://doi.org/10.1016/j.rser.2017.07.009>
- Agyenim, F., Hewitt, N., Eames, P., & Smyth, M. (2010). A review of materials, heat transfer and phase change problem formulation for latent heat thermal energy storage systems (LHTESS). *Renewable and Sustainable Energy Reviews*, 14(2), 615–628. <https://doi.org/10.1016/j.rser.2009.10.015>
- ASTM C1784-14. (2015). Standard Test Method for Using a Heat Flow Meter Apparatus for Measuring Thermal. *ASTM International*, 1–17. <https://doi.org/10.1520/C1784-20.2>
- Baetens, R., Jelle, B. P., & Gustavsen, A. (2010). Phase change materials for building applications: A state-of-the-art review. *Energy and Buildings*, 42(9), 1361–1368. <https://doi.org/10.1016/j.enbuild.2010.03.026>
- Bland, A., Khzouz, M., Statheros, T., & Gkanas, E. I. (2017). PCMs for residential building applications: A short review focused on disadvantages and proposals for future development. *Buildings*, 7(3). <https://doi.org/10.3390/buildings7030078>
- Cabeza, L. F., Castell, A., Barreneche, C., Gracia, A. De, & Fernández, A. I. (2011). Materials used as PCM in thermal energy storage in buildings: A review. *Renewable and Sustainable Energy Reviews*, 15(3), 1675–1695. <https://doi.org/10.1016/j.rser.2010.11.018>
- DFROBOT. (2022). Thin film pressure sensors. Retrieved from [https://media.digikey.com/pdf/Data\\_Sheets/DFRobot\\_PDFs/SEN0293\\_Web.pdf](https://media.digikey.com/pdf/Data_Sheets/DFRobot_PDFs/SEN0293_Web.pdf)
- Fang, X., Fan, L. W., Ding, Q., Yao, X. L., Wu, Y. Y., Hou, J. F., ... Hu, Y. C. (2014). Thermal energy storage performance of paraffin-based composite phase change materials filled with hexagonal boron nitride nanosheets. *Energy Conversion and Management*, 80, 103–109. <https://doi.org/10.1016/j.enconman.2014.01.016>
- Fauzi, H., Metselaar, H. S. C., Mahlia, T. M. I., & Silakhori, M. (2014). Sodium laurate enhancements the thermal properties and thermal conductivity of eutectic fatty acid as phase change material (PCM). *Solar Energy*, 102, 333–337. <https://doi.org/10.1016/j.solener.2013.07.001>
- Instruments, T. A. (2022). *Fox Instruments* (p. Sampled 2/22). p. Sampled 2/22. Retrieved from <https://www.tainstruments.com/products/thermal-conductivity-meter/lasercomp-heat-flow-meters/>
- Kalapala, L., & Devanuri, J. K. (2018). Influence of operational and design parameters on the performance of a PCM based heat exchanger for thermal energy storage – A review. *Journal of Energy Storage*, 20(September), 497–519. <https://doi.org/10.1016/j.est.2018.10.024>
- Kalnæs, S. E., & Jelle, B. P. (2015). Phase change materials and products for building applications: A state-of-the-art review and future research opportunities. *Energy and Buildings*, 94(7491), 150–176. <https://doi.org/10.1016/j.enbuild.2015.02.023>
- Kamali, S. (2014). Review of free cooling system using phase change material for building. *Energy and Buildings*, 80, 131–136. <https://doi.org/10.1016/j.enbuild.2014.05.021>
- Kenisarin, M. M. (2014). Thermophysical properties of some organic phase change materials for latent heat storage. A review. *Solar Energy*, 107, 553–575. <https://doi.org/10.1016/j.solener.2014.05.001>
- Khadiran, T., Hussein, M. Z., Zainal, Z., & Rusli, R. (2016). Advanced energy storage materials for building applications and their thermal performance characterization: A review. *Renewable and Sustainable Energy Reviews*, 57, 916–928. <https://doi.org/10.1016/j.rser.2015.12.081>
- Lachheb, M., Karkri, M., Albouchi, F., Mzali, F., & Nasrallah, S. Ben. (2014). Thermophysical properties estimation of paraffin/graphite composite phase change material using an inverse method. *Energy Conversion and Management*, 82, 229–237. <https://doi.org/10.1016/j.enconman.2014.03.021>
- Lin, W., Zhang, W., Ling, Z., Fang, X., & Zhang, Z. (2020). Experimental study of the thermal performance of a novel plate type heat exchanger with phase change material. *Applied Thermal Engineering*, 178, 115630. <https://doi.org/https://doi.org/10.1016/j.applthermaleng.2020.115630>
- Mahvi, A., & Woods, J. (2020). *Designing Thermal Energy Storage Devices using the Ragone Framework Past Work on Phase-Change Thermal Storage Materials*.
- Mavrigiannaki, A., & Ampatzi, E. (2016). Latent heat storage in building elements: A systematic review on

- properties and contextual performance factors. *Renewable and Sustainable Energy Reviews*, 60, 852–866. <https://doi.org/10.1016/j.rser.2016.01.115>
- Mehrali, M., Tahan Latibari, S., Mehrali, M., Mahlia, T. M. I., Sadeghinezhad, E., & Metselaar, H. S. C. (2014). Preparation of nitrogen-doped graphene/palmitic acid shape stabilized composite phase change material with remarkable thermal properties for thermal energy storage. *Applied Energy*, 135, 339–349. <https://doi.org/10.1016/j.apenergy.2014.08.100>
- Merlin, K., Delaunay, D., Soto, J., & Traonvouez, L. (2016). Heat transfer enhancement in latent heat thermal storage systems: Comparative study of different solutions and thermal contact investigation between the exchanger and the PCM. *Applied Energy*, 166, 107–116. <https://doi.org/10.1016/j.apenergy.2016.01.012>
- Peng, S., Fuchs, A., & Wirtz, R. A. (2004). Polymeric phase change composites for thermal energy storage. *Journal of Applied Polymer Science*, 93(3), 1240–1251. <https://doi.org/10.1002/app.20578>
- Rahimi, M., Ranjbar, A. A., Ganji, D. D., Sedighi, K., Hosseini, M. J., & Bahrampoury, R. (2014). Analysis of geometrical and operational parameters of PCM in a fin and tube heat exchanger. *International Communications in Heat and Mass Transfer*, 53, 109–115. <https://doi.org/10.1016/j.icheatmasstransfer.2014.02.025>
- Singh, P., Sharma, R. K., Ansu, A. K., Goyal, R., Sarı, A., & Tyagi, V. V. (2021). A comprehensive review on development of eutectic organic phase change materials and their composites for low and medium range thermal energy storage applications. *Solar Energy Materials and Solar Cells*, 223(December 2020), 110955. <https://doi.org/10.1016/j.solmat.2020.110955>
- Souayfane, F., Fardoun, F., & Biwole, P. H. (2016). Phase change materials (PCM) for cooling applications in buildings: A review. *Energy and Buildings*, 129, 396–431. <https://doi.org/10.1016/j.enbuild.2016.04.006>
- Tyagi, V. V., & Buddhi, D. (2007). PCM thermal storage in buildings: A state of art. *Renewable and Sustainable Energy Reviews*, 11(6), 1146–1166. <https://doi.org/10.1016/j.rser.2005.10.002>
- Woods, J., Mahvi, A., Goyal, A., Kozubal, E., Odukomaiya, A., & Jackson, R. (2021). Rate capability and Ragone plots for phase change thermal energy storage. *Nature Energy*, 6(3), 295–302. <https://doi.org/10.1038/s41560-021-00778-w>
- Woods, J., Mahvi, A., Goyal, A., Kozubal, E., & Odukomaiya, W. (2019). *An air conditioner with composite phase change material ( FY19 Technology Commercialization Fund project ) Budget :*
- Wu, J., Feng, Y., Liu, C., & Li, H. (2018). Heat transfer characteristics of an expanded graphite/paraffin PCM-heat exchanger used in an instantaneous heat pump water heater. *Applied Thermal Engineering*, 142, 644–655. <https://doi.org/https://doi.org/10.1016/j.applthermaleng.2018.06.087>
- Yang, L., Yan, H., & Lam, J. C. (2014). Thermal comfort and building energy consumption implications - A review. *Applied Energy*, 115, 164–173. <https://doi.org/10.1016/j.apenergy.2013.10.062>
- Youssef, W., Ge, Y. T., & Tassou, S. A. (2018). CFD modelling development and experimental validation of a phase change material (PCM) heat exchanger with spiral-wired tubes. *Energy Conversion and Management*, 157, 498–510. <https://doi.org/10.1016/j.enconman.2017.12.036>

## ACKNOWLEDGEMENT

The authors would like to acknowledge the Buildings Technology Office and Sven Mumme at the Department of Energy for their support in this work. Also, the Building Technologies Integration and Research Center at Oak Ridge National Lab for use of the HFMA and general support.